Proceedings of the ASME 2010 29th International Conference on Ocean, Offshore and Arctic Engineering
OMAE2010
June 6-11, 2010, Shanghai, China

OMAE2010-21043

RE-EVALUATION OF VIV RISER FATIGUE DAMAGE

Yahya Modarres-Sadeghi
MIT/UMass
Cambridge/Amherst, MA, USA

Rémi Bourguet
MIT
Cambridge, MA, USA

Michael S Triantafyllou
MIT
Cambridge, MA, USA

Michael Tognarelli
BP America Production Co.
Houston, TX, USA

Pierre Beynet
BP America Production Co.
Houston, TX, USA

ABSTRACT

The paper describes a new characterization of the properties of the vortex-induced vibrations (VIV) of marine risers, which emerges from processing field and experimental data. We show that two currently employed assumptions: (a) that VIV is a statistically steady-state response containing one or several frequencies, and (b) that VIV consists of alternating dominant modes (mode-sharing), are inadequate. Instead, we find that the response either contains strong traveling wave components accompanied by high force harmonics; or consists of a chaotic wandering among several traveling and standing waves, associated with a wide-band spectrum; both types of response require careful consideration for correct fatigue evaluation.

INTRODUCTION

Marine risers and mooring lines placed in cross-flow may exhibit high frequency, vortex-induced vibrations accompanied by significant drag increase; this constitutes an important problem for ocean applications, especially for deep water oil exploration and production.

The problem of vortex-induced vibrations (VIV), even in its simplest form of a flexibly mounted rigid cylinder in cross-flow, is so complex that a complete characterization of its properties as function of the Reynolds number still eludes us. As a result, the vortex-induced vibration of rigid cylinders has become the canonical problem for bluff body-flow interaction, and has been studied extensively, as reviewed in Bearman (1984), Vandiver (1993), Sarpkaya (2004), and Williamson and Govardhan (2004).

In previous studies of the VIV of rigid and flexible cylinders, a statistically stationary region of the signal was typically identified and VIV was treated either as a periodic phenomenon or as a statistically steady-state random response. The spectrum of the oscillations contained fundamental frequencies close to the Strouhal frequency. In some cases higher harmonics of force are also present, with additional spectral peaks at 3 and 5 times the fundamental frequency (Dahl et al. 2006, 2007). The rationale for omitting regions of transient response was the assumption that VIV settles in steady-states and contains non-stationary response only during the initial transients, or when external changes in forcing, especially current speed and direction, force a change in the state of the system. Mode-switching, the phenomenon whereby there is a sudden and marked change in the features of VIV response, including its amplitude and frequency, was presumed to be an isolated phenomenon, prompted by external changes in the flow.

We show in this paper, however, that there are long periods of VIV response that can be characterized as statistically non-stationary, having a wide-band power spectrum, which also contains several frequencies in addition to the Strouhal frequency. Random switching from stationary to non-stationary response, and vice-versa, is frequent and constitutes a principal feature of riser response. We can observe this switching by subdividing the signal into smaller time segments and obtain their power spectra. In addition, we correlate the observed responses with associated wake pattern obtained through direct numerical simulations performed at low and moderate Reynolds numbers.

ANALYSIS OF FIELD AND EXPERIMENTAL DATA

We used the experimental data from the Norwegian Deepwater Programme (NDP) Riser High Mode VIV tests (Braaten and Lie, 2004; Trim et al., 2005), DeepStar Gulf Stream (Marcollo et al., 2007), as well as data from an experimental work by Chaplin et al. (2005), in order to investigate the signal behavior.

Figure 1 shows the time history, power spectral density, phase-plane plot and Poincaré map of a rare case of the NDP data which was specifically selected to exhibit the statistically stationary response that is typically expected to occur: The signal shows a sharp fundamental frequency at 1.5 Hz and a 3rd harmonic component at 4.5 Hz. The 1st and the 3rd harmonic peaks are easily identified in the power spectral density (PSD) plot, while there are three clustered points in the Poincaré map which represent a period-3 oscillation. The response is not purely periodic and can be characterized as quasi-periodic, as also evidenced by the donut-like phase plane.

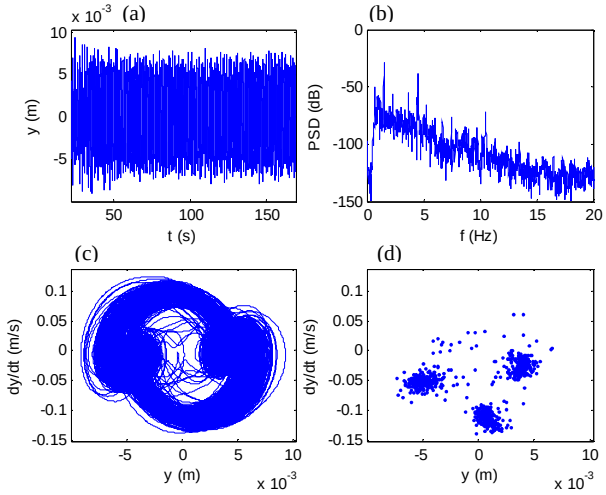

Figure 1: (a) Time history, (b) PSD plot, (c) phase plane, and (d) Poincaré map of the entire signal at a point along the length of the riser, case 2310, with a linearly sheared flow profile, U_{max}=0.3 m/s, showing steady-state VIV behavior; this is rare.

In Figure 2 we show a more commonly occurring response, exhibiting features of a chaotic signal: The time history does not show periodicity, while the PSD plot shows an underlying broad-band spectrum (in contrast to the PSD plot of Figure 1); the trajectories tend to fill up a region in phase plane, and the Poincaré map shows a cloud of points. As we show in the following sections, the majority of VIV responses present a behavior similar to that shown in Figure 2. A reliable method of proving chaotic response is to calculate the Lyapunov exponent, an index of the sensitivity of chaotic oscillations to initial conditions. There are several procedures to calculate Lyapunov exponent (see, e.g., Wolf et al., 1985); however, their use for experimental time series is not reliable (Moon, 1992).

The PSD plot of a chaotic oscillation shows a broad band spectrum with no significant 3rd or 5th harmonic peaks; hence this represents a different situation than for periodic VIV. The third and firth harmonics compared to the fundamental (Strouhal) frequency are small, and yet a wide band of frequencies, which include these higher harmonics, must be considered as a frequency-distributed response.

In some instances, the entire measured signal may be found to be either quasi-periodic or chaotic; however, it is more common that the signal contains parts pertaining to both types of response, with clear switching times between the two types. For example, in case 2430, the motion is chaotic for the segment t=[13-20]s, but becomes quasi-periodic for the segment t=[27-33]s. Figure 3(a) shows the scalogram of the entire time history for case 2430. A switching is observed clearly in this figure; for t= [0-12]s the peaks of the scalogram are widely spread, while for t>12s, a large peak at the 1st harmonic accompanied by a large peak at the 3rd harmonic component are observed. These large peaks correspond to a mainly periodic motion.

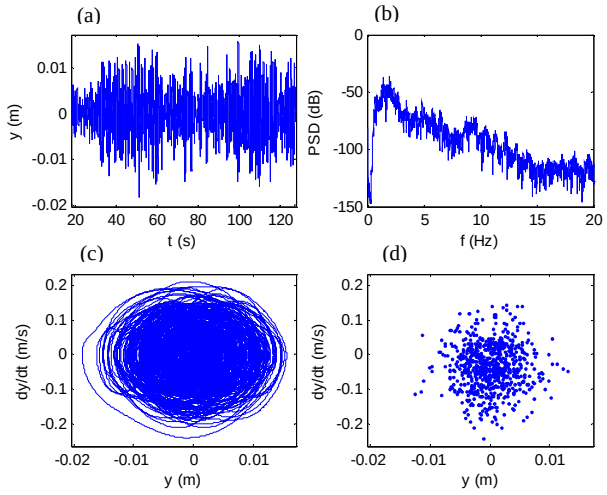

Figure 2: The entire signal at a specific point along the riser, for case 2320, a linearly sheared flow case, showing chaotic behavior in field tests.

In summary, and for the NDP sheared cases, there are 5 purely chaotic signals and 1 purely quasi-periodic one. In the majority of these signals, however, the oscillations switch from quasi-periodic to chaotic and vice versa, as is observed, e.g., in case 2420 (U_{max}=1.4 m/s), when the signal is quasi-periodic for t~11-18 and t~22-25 and chaotic for t<11 and 18<t<22. The scalogram of this signal (Figure 3(b)) shows how wide-spread peaks are observed in the chaotic region and narrow-banded large peaks in periodic regions.

We have analyzed results from the DeepStar Gulf Stream data (Marcollo et al., 2007), as well as the experimental data by Chaplin et al. (2005), in order to establish that the behavior we

have observed in the NDP data is not limited to this particular set of experiments. In general, we have observed a behavior very similar to what we have discussed for NDP tests: A combination of chaotic and periodic regions exist versus time and space for all the cases studied here. Figure 4(a) shows a scalogram of a sample DeepStar case, where the signal shows chaotic behavior. In Figure 4(b), which is a sample case of the Chaplin et al. data, a large peak is observed for t<10 s, then there is a period of low-amplitude peaks for 10<t<30, followed by a return to large peaks for t>30 s, clearly showing a switching between a periodic motion and a chaotic one.

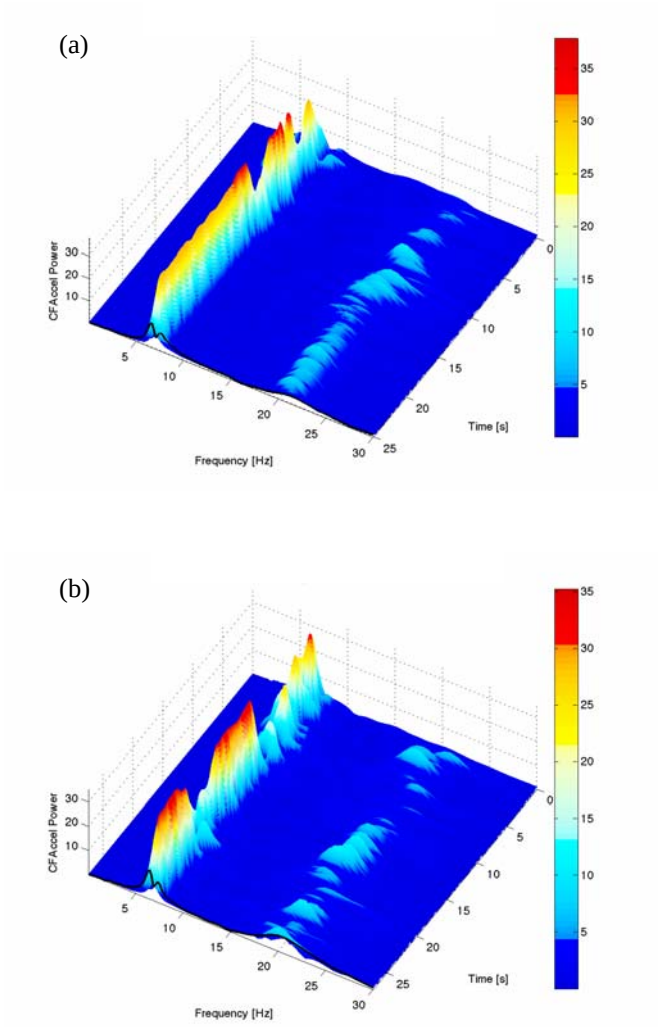

Figure 3 Scalogram of the entire signal for (a) case 2430, and (b) case 2420 of the NDP data.

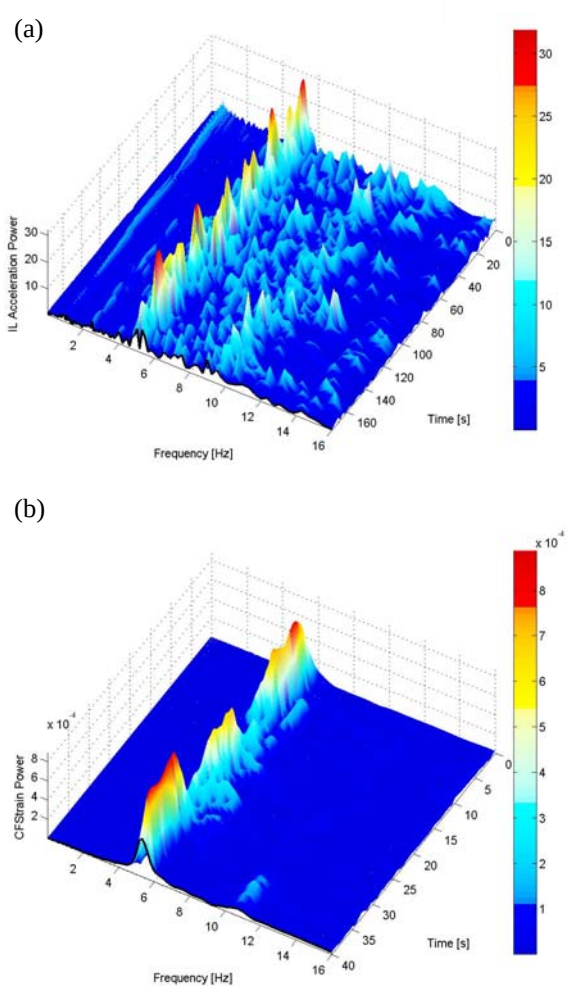

Figure 4 Scalogram of (a) a sample case from DeepStar experiments, and (b) a sample case from Chaplin et al. (2005) experiments

IMPACT ON FATIGUE DAMAGE

In this section some fatigue calculations are conducted to assess the impact of each type of riser response. In order to calculate the fatigue life of the riser, an S-N curve of the form $N=A(1/S)^B$ is used, where N is the number of cycles, S is stress range in MPa, $A = 4.8641\times10^{11}$ and $B = 3.00$ (see Trim et al., 2005). Fatigue life calculations are conducted based on rainflow fatigue prediction method (Christian, 2002).

If a VIV signal contains large third and fifth harmonic components, the fatigue damage can be orders of magnitude larger than fatigue damage calculated based on using only the first harmonic (Strouhal frequency) signal (Modarres-Sadeghi et al., 2010). As discussed previously, chaotic signals have relatively small third and fifth harmonic components. As an example, the 3rd harmonic component of the strain for case 2480, a sheared flow case with U_{max} = 2 m/s, is 0.05 of the total strain (3rd harmonic component is defined as the area under the 3rd harmonic peak in the PSD plot divided by the total area).

One could then argue that because this is a negligible higher harmonic component, we can consider only frequencies near the Strouhal frequency. If this is done, however, the resulting fatigue damage will be under-predicted by 70%, as the filtered strain provides a fatigue damage of 7.2×10^{-6} 1/years, while the actual fatigue damage is 2.4×10^{-5} 1/years. Hence, in general, it is not safe to use the filtered part of the strain (around the Strouhal frequency) in order to calculate fatigue damage, even when the third high strain harmonics are small, because the signal may be chaotic. The difference between fatigue life calculated using a filtered VIV signal and the actual fatigue life is large when the signal is chaotic, because the spectrum is broad-band.

A major difference between the fatigue calculation of a quasi-periodic and a chaotic signal is the impact of filtering: A fatigue calculation for a quasi-periodic[1] response is practically independent of the filter used, since most energy is concentrated around the Strouhal frequency, while the corresponding response for a chaotic response[2] depends highly on filtering limits. To demonstrate this, we have chosen two different responses that have comparably small 3rd harmonic strain components (around 0.03 of the total strain, for both cases); however, interval 1 is chaotic, while interval 2 is periodic. Table 1 gives a summary of fatigue life calculations using various frequency bands to filter the signals. For chaotic responses the fatigue life predictions vary substantially with the filter frequency band used, while for periodic signals fatigue damage prediction is independent from any filter used. An interesting observation is that in this particular case the actual fatigue damage calculated using the periodic interval is approximately equal to the actual damage calculated using the chaotic interval. The reason is that the periodic strain signal has much higher amplitude at the Strouhal frequency, but the chaotic strain signal has lower amplitude, but significant energy spread over a wider frequency range.

NUMERICAL SIMULATIONS

Direct numerical simulations of the flow past a long flexible cylinder have been performed at low and moderate Reynolds numbers to investigate the effect of the structural response on the wake patterns. A cylindrical tensioned beam of aspect ratio 200 and mass ratio 6 is subjected to a sheared oncoming cross-flow. The mass ratio is defined as $\rho_s/\rho_f D^2$ where ρ_s is the beam density per unit length, ρ_f the fluid density and D the beam diameter. The structure is pinned at both ends and is free to vibrate in the in-line and cross-flow directions. A linear structural model is used and the flow is modeled by the Navier-Stokes equations under incompressibility assumption. The coupled fluid-structure problem is solved by the Nektar code, based on the spectral/hp elements method (Karniadakis and Sherwin, 1999). Validation studies of the numerical method have been carried out in previous works studying similar riser configurations (Newman and Karniadakis, 1997; Evangelinos and Karniadakis, 1999; Lucor et al., 2001).

Table 1: Fatigue damage values (in 1/years) for interval 1 (chaotic) and interval 2 (periodic) of case 2490.

	Fatigue damage	Filtered fatigue damage; frequency band: [9.3 10.3] Hz	Filtered fatigue damage; frequency band: [8.8 10.8] Hz
Chaotic	4.3×10^{-5}	0.7×10^{-5}	1.4×10^{-5}
Periodic	4.8×10^{-5}	4.8×10^{-5}	4.8×10^{-5}

The oncoming flow is linearly sheared with a shear parameter (Vandiver et al., 1996) equal to 1.14, while the non-dimensional inflow velocity varies from 0.3 to 1.1. Three Reynolds number ranges are considered: $Re \in [30,110]$, $Re \in [90,330]$ and $Re \in [300,1100]$. These Reynolds numbers are based on the cylinder diameter and the local oncoming velocity. Figure 5 shows instantaneous iso-surfaces of spanwise vorticity downstream of the cylinder. The shear flow results in variation of the fundamental frequency of the von Kármán instability along the span, causing a strong modulation of the wake patterns. Multiple vortex shedding frequencies are observed along the span. Regions of regular vortex shedding are separated by intermediate zones of reconnection between vortex filaments. In addition, a large region of the wake is characterized by oblique vortex shedding.

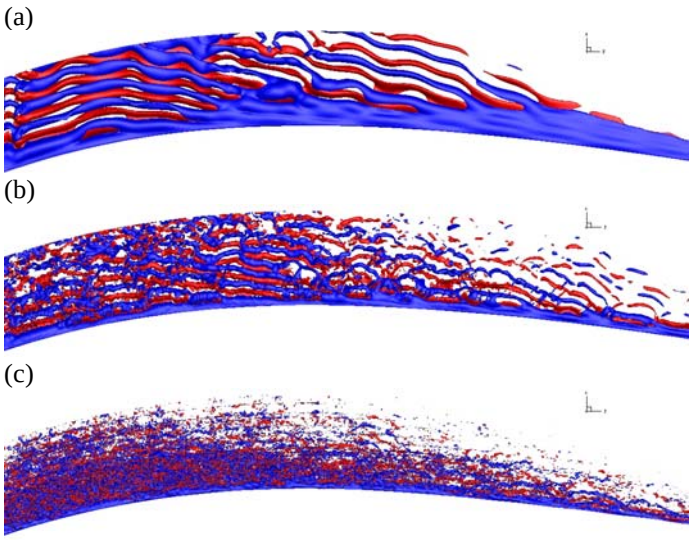

Figure 5: Instantaneous iso-surfaces of z vorticity for (a) $Re \in [30,110]$, $\omega_z=\pm0.2$, (b) $Re \in [90,330]$, $\omega_z=\pm0.4$ and (c) $Re \in [300,1100]$, $\omega_z=\pm1.2$. High oncoming velocity is on the left and the flow is from bottom to top. Only a part of the downstream domain is shown.

Temporal evolutions of the structure responses in the in-line and cross-flow directions for the case $Re \in [300,1100]$ are

[1] A signal with many peaks in the PSD plot, when all the peaks can be re-written as algebraic summations of two fundamental frequencies.

[2] A signal with broad-band PSD plots.

presented in Figure 6. The in-line response has been centered about the mean deviation of the cylinder. In both directions, structural motions mainly consist of modulated traveling waves, except near the ends where a standing wave pattern dominates. For this case, the maximum displacement amplitudes in the in-line and cross-flow directions are 0.07 and 0.8 cylinder diameters, respectively.

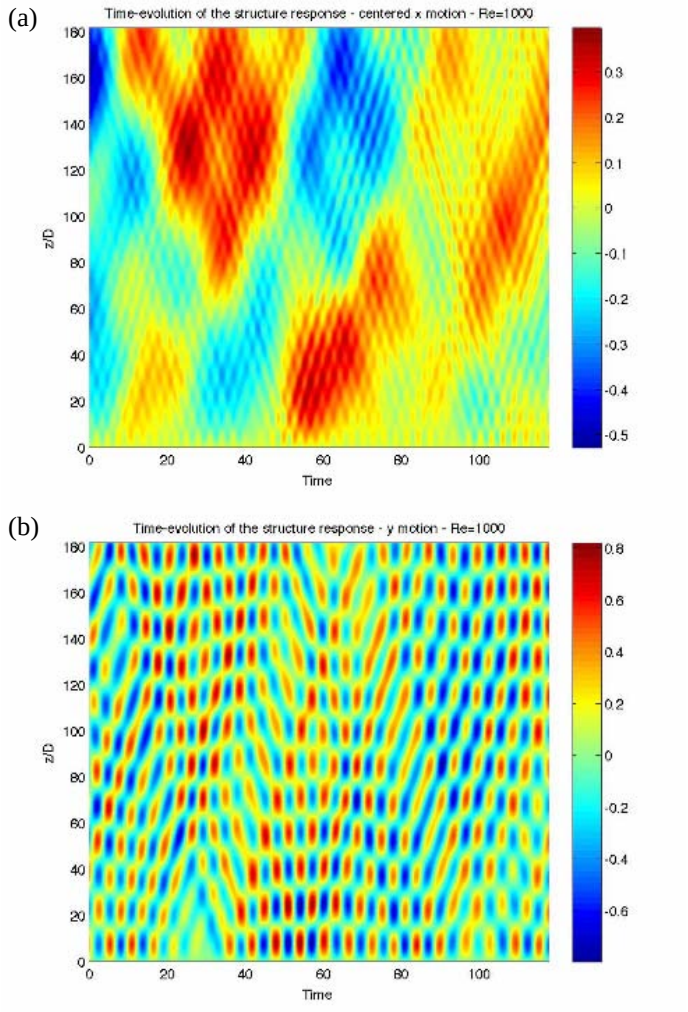

Figure 6: Temporal evolution of the structural response along the span in (a) the in-line and (b) the cross-flow directions, for the case Re ∈ [300,1100]. The in-line motion has been centered about the cylinder mean position.

Spanwise evolution of the temporal spectra associated with the in-line and cross-flow responses are shown in Figure 7, for the same case. The structure exhibits multi-frequency response in the in-line direction. An analysis of the in-line evolution of each temporal mode phase shows that most of the predominant modes are associated with responses traveling from high to low velocity regions but that only few are traveling towards the high velocity region. A single wave response, traveling toward the low velocity region, dominates the structural response in the cross-flow direction. The predominant structural modes excited in the in-line and cross-flow directions are the 23rd and the 13th, respectively, for all cases. The preferential direction of the structural response, traveling from high to low cross-flow velocity regions, is closely related to the previously mentioned oblique shedding pattern and, more generally, to the form of the near wake vortical patterns induced by the sheared flow.

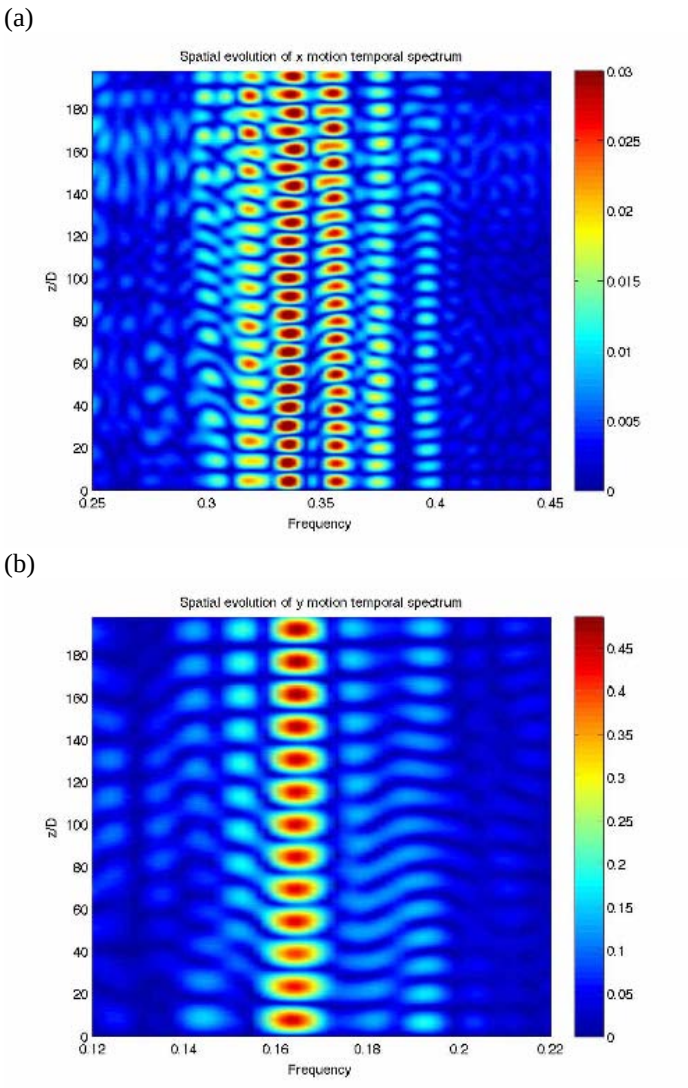

Figure 7: Spanwise evolution of structure response temporal spectra in (a) the in-line and (b) the cross-flow directions, for the case Re ∈ [300,1100].

The predominant vibration frequencies are almost constant along the span (Figure 7), despite the fact that the vortex shedding frequency is significantly modulated. For the three simulations shown, lock-in is observed in the high velocity region, and its spanwise extent is 30-40% of the total cylinder

length. As a consequence, within this lock-in region, the vortex shedding frequency can be driven relatively far from the Strouhal frequency which would be measured in the wake of a stationary cylinder. As an example, in the case of Re $\in$ [300,1100], the non-dimensional vortex shedding frequency varies between 0.15 and 0.22 within the lock-in region. In the region where the structural oscillations and vortex shedding are not synchronized, structural vibration amplitudes remain similar to those occurring within the lock-in region, even though the flow-structure interaction acts mainly as a damping mechanism.

DISCUSSION

For flexible structures placed in sheared cross-flow, the Strouhal frequency varies along the length. This provides a wide range of potential modes which may be excited, and increases the likelihood of chaotic response. There is a counter-balancing effect, however: In a sheared flow, the riser structural response contains a large component of traveling waves, as energy is input in regions of high current velocity and then transferred and dissipated in regions of low velocity. Newman and Karniadakis (1996, 1997) and Lucor et al. (2001) were among the first to demonstrate clearly the presence of standing and traveling waves in the case of a vibrating flexible cable. As the riser length increases, standing waves become a very small part of the overall response, while vortex formation is also in the form of a traveling wave, resulting in a substantial increase in correlation length.

Hence there are two possible states of response for the riser:

- The first condition consists of several competing modes with closely spaced frequencies. The vortex formation pattern and the riser response wander randomly through various modes; the frequency undergoes step changes, although two or more frequencies may coexist for part of the time. The modes corresponding to each frequency are not the free vibration modes, but are a mixture of traveling and standing waves; each mode may be excited from a different location along the riser, depending on the local current velocity and the corresponding local Strouhal frequency.
- The second condition is that of a nearly monochromatic response, consisting principally of traveling waves in one direction, which dominate the entire VIV. The reason for this dominance is a dual resonance, in the in-line and transverse directions, respectively, over a substantial part of the riser length, which enhances correlation and causes a very repeatable orbit at each point of the riser, accompanied by multi-vortex formation and hence strong third and fifth force harmonics.

Transition from one type of response to the other was found in the majority of the field cases considered. Transition typically started at one end of the riser and propagated over the entire riser length.

CONCLUSIONS

An analysis of field and experimental data recording the vortex-induced vibrations of marine risers in shear currents shows that the response switches randomly between two types of response: A statistically stationary response whose spectrum contains either a single or multiple peaks, possibly including high harmonics of the Strouhal frequencies; and a response that switches unpredictably among a number of frequencies and has all the characteristics of a chaotic response with a wide-band spectrum. Both types of responses are found for risers in sheared and uniform currents; relatively small changes in the incoming current velocity can bring large changes in the type of response, with potentially significant impact on the fatigue damage. A proper fatigue damage calculation must account for the type of VIV response. Direct numerical simulations, at low and moderate Reynolds numbers, of the flow past a long flexible cylinder relate the observed structural responses to the vortical patterns in the wake.

ACKNOWLEDGEMENTS

The authors acknowledge with gratitude the permission granted by the Norwegian Deepwater Programme (NDP) Riser and Mooring Project to use the Riser High Mode VIV tests. Financial support was provided by the BP-MIT Major Projects Program, and BP America Production Co. The authors are grateful to Professor John Chaplin of the University of Southampton for providing them with his detailed experimental data.

REFERENCES

Bearman, P.W., 1984. Vortex shedding from oscillating bluff bodies, *Annual Review of Fluid Mechanics*, **16**, 195-222.

Braaten, H., Lie, H., 2004. NDP riser high mode VIV tests. Main report No. 512394.00.01, *Norwegian Marine Technology Research Institute.*

Chaplin, J.R., Bearman, P.W., Huera Huarte, F.J., Pattenden, R.J., 2005. Laboratory measurements of vortex-induced vibrations of a vertical tension riser in a stepped current. *Journal of Fluids and Structures* **21**, 3–24.

Christian, L., 2002. *Mechanical vibration and shock*. Volume 4. New York, NY: Taylor and Francis.

Dahl, J.M., Hover, F.S., Triantafyllou, M.S., 2006. Two-degree-of-freedom vortex-induced vibrations using a force assisted apparatus. *Journal of Fluids and Structures* **22**, 807-818.

Dahl, J.M., Hover, F.S., Triantafyllou, M.S., Dong, S., Karniadakis, G.E., 2007. Resonant vibrations of bluff bodies cause multi-vortex shedding and high frequency forces, *Physical Review Letters* **99**, 144503.

Evangelinos, C., Karniadakis, G.E., 1999. Dynamics and flow

structures in the turbulent wake of rigid and flexible cylinders subject to vortex-induced vibrations. *Journal of Fluid Mechanics* **400**, 91–124.

Karniadakis, G.E, Sherwin, S.J., 1999. *Spectral/hp Element Methods for CFD*. Oxford University Press.

Lucor D., Imas L., Karniadakis G.E. 2001. Vortex dislocations and force distribution of long flexible cylinders subjected to sheared flows. *Journal of Fluids and Structures* **15**, 641-650.

Marcollo, H., Chaurasia H. and Vandiver J. K., "Phenomena Observed in VIV Bare Riser Field Tests", Proceedings of OMAE2007, OMAE2007-29562

Modarres-Sadeghi, Y., Mukundan, H., Dahl, J.M., Hover, F.S., Triantafyllou M.S., 2010. The Effect of Higher Harmonic Forces on Fatigue Life of Marine Risers. *Journal of Sound and Vibration*, **329**, 43-55..

Moon, F.C., 1992. *Chaotic and fractal dynamics: An introduction for applied scientists and engineers*. New York: John Wiley and Sons.

Newman, D.J., Karniadakis, G.E., 1996. Simulations of flow over a flexible cable: comparison of forced and flow induced vibration. *Journal of Fluids and Structures* **10**, 439–453.

Newman, D.J., Karniadakis, G.E., 1997. Simulations of flow past a freely vibrating cable. *Journal of Fluid Mechanics* **344**, 95–136.

Sarpkaya, T., 2004. A Critical Review of the Intrinsic Nature of Vortex-Induced Vibrations. *Journal of Fluids and Structures*. **19**, 389-447.

Trim, A.D., Braaten, H., Lie, H., Tognarelli, M.A., 2005. Experimental Investigation of Vortex-Induced Vibration of Long Marine Risers. *Journal of Fluids and Structures*. **21**, 335-361.

Vandiver, J.K., 1993. Dimensionless Parameters Important to the Prediction of Vortex-Induced Vibration of Long, Flexible Cylinders in Ocean Currents. *Journal of Fluids and Structures*. **7**, 423-455.

Vandiver, J.K., Allen, D., Li, L., 1996. The occurrence of lock-in under highly sheared conditions. *Journal of Fluids and Structures*. **10**, 555-561.

Williamson, C.H.K, Govardhan R., 2004, Vortex-Induced Vibrations. *Annual Review of Fluid Mechanics* **36**, 413-455.

Wolf, A., Swift, J.B., Swinney, H.L., Vasano J.A., 1985. Determining Lyapunov exponents from a time series. *Physica* **16D**, 285-317.